Electrical Power and Energy Systems 116 (2020) 105523

Contents lists available at ScienceDirect

Electrical Power and Energy Systems

journal homepage: www.elsevier.com/locate/ijepes

A look-ahead dispatch method accounting for improved primary frequency response

Jianhua Chen[a,*], Yao Zhang[b]

[a] State Grid Jibei Electric Power Company Ltd., Xicheng District, Beijing, China
[b] China Nuclear Power Engineering Company Ltd., Haidian District, Beijing, China

A B S T R A C T

It is becoming more and more important to consider the frequency security of power system during active power dispatch, especially when large-scale wind power is integrated. This paper describes a robust look-ahead dispatch method accounting for improved primary frequency response, in which a proportional-differential controller is introduced into the conventional primary frequency control as feedback function. And an order reduction method for frequency-domain transfer function is proposed. Based on this, the time-domain frequency response characteristic is derived and incorporated into the robust look-ahead dispatch model. The simulation results on IEEE RTS system proved the effectiveness of the proposed method on improving the frequency response characteristics and increasing the penetration level of renewable resources.

1. Introduction

Wind energy is one of the most promising renewable energy sources in the future, which is inexhaustible, clean and pollution-free. And the global wind power generation industry has achieved extraordinary development in the past two decades. In China, the new installed wind turbine capacity was 19,660 MW at the end of 2017, which accounts for 37.45% of the world's new installed capacity and ranks first in the world [1].

Although there are many advantages for wind energy, it is also highly intermittent and stochastic. Large-scale wind power integration brings great challenges to the active power dispatch and frequency control of power system. When an unexpected wind power fluctuation happens, the active power balance of the power system will be broken and the frequency will deviate from its nominal value correspondingly, which makes the power system unstable. What's more, most of the wind turbines are asynchronous generators, who cannot provide inertial response and primary frequency control services to the system like traditional synchronous generators, and thus making the system frequency control more difficult.

Look-ahead dispatch method, a receding horizontal based dynamic dispatch method, has been proved to be an effective method to improve the utilization of renewable energy resources and has been much studied in previous literature [2–8]. Based on the predictive output from the wind power, the look-ahead dispatch algorithm for dispatching the available generation resources is presented in [2]. The simulation results show that the look-ahead dispatch could lower the generation costs by directly dispatching the generator output from the renewable resources in order to compensate temporal load variations over predefined time horizon. [3] presents a method for the early detection and optimal corrective measures of power system insecurity in an enhanced look-ahead dispatch framework. [4] presents a case study of applying look-ahead dispatch in the nodal market operations of Electric Reliability Council of Texas system. A new look-ahead multi-timeframe generator control and dispatch method was developed in [5] in the PJM real time system to determine the optimal dispatch solutions for each generator. In [6], two models are presented to incorporate short-term stored energy resources into multiple-interval real time look-ahead security constrained economic dispatch (SCED). Study on a three-bus system indicates that using multiple-interval SCED can reduce the market clearing cost. In [7], a linear programming approach is applied to the look-ahead dispatch of grid-tied microgrids with energy storage, demand response resources and non-dispatchable solar or wind resources. The price responsive demand study is specifically designed in [8] to evaluate the impact of price responsive demand program on many aspects of PJM look-ahead system operations and market clearing, including resource dispatch, security constraint management, and energy pricing, particularly in shortage pricing context.

Although the uncertainty from intermittent resources has been considered in look-ahead dispatch, the power system may still suffer capacity inadequacy when wind power output deviates from the predicted value. Hence, the robust optimization is introduced into the conventional look-ahead dispatch method, in which the uncertainty of wind power output is considered as an interval, and the optimal

* Corresponding author.
E-mail address: dffg111@163.com (J. Chen).

https://doi.org/10.1016/j.ijepes.2019.105523
Received 28 June 2019; Received in revised form 31 July 2019; Accepted 1 September 2019

solution is immunized against all realizations of the uncertain data within in the interval [9–13]. A robust interval look-ahead power dispatch model is proposed in [10], which gives interval solutions for wind farms and optimal economic solutions for conventional units to mitigate the uncertainty inherent to wind power. An adjustable uncertainty set is proposed in [11] to reduce the conservativeness of robust look-ahead dispatch. Test results show that the method is effective in reducing the conservativeness and ensuring system security with controllable risk. A flexible look-ahead dispatch model is developed in [12] to balance the operational costs and the conditional value-at-risk of wind power based on robust optimization. An adaptive robust optimization model with dynamic uncertainty sets for the economic dispatch of power systems with high level of wind penetration is presented in [13].

To guarantee the power system stability, the post-fault frequency evolution should be accounted for in the robust look-ahead dispatch model. However, despite many studies on look-ahead dispatch method and model for large-scale wind power integrated power system, only few of them account for the frequency stability issues [14–18]. In [14], a co-optimized market clearing algorithm is presented that incorporates two new frequency-based security constraints: the rate of change of frequency constraint, and the minimum frequency constraint. In [15], a modified system frequency response model is derived and used to find analytical representation of system minimum frequency in thermal-dominant multi-machine systems. The contribution of the demand side and variable-speed wind turbines to the primary frequency control is analysed in [16]. In [17], a unit commitment model that simultaneously accounts for both primary and tertiary reserve constraints is formulated. [18] proposes a stochastic unit commitment formulation accounting for post-fault dynamic frequency requirement, which could ensure the dynamic evolution of post-fault frequency to be within limits associated with the RoCoF, nadir frequency and quasi-steady-state frequency.

It can be observed that the previous studies are mainly focused on the method to incorporate frequency-based security constraints into look-ahead dispatch model. However, for those power systems with large-scale wind power integration, when the frequency security constraints are considered in real-time operation, the wind power output will be abandoned severely, making the dispatch result very conservative, which is quite not economical and not the expectation of operators. Hence, the method that could effectively improve the frequency response characteristics in economic dispatch is needed.

This paper proposes a robust look-ahead dispatch method accounting for improved primary frequency response, in which a proportional-differential controller (PD) as feedback function is designed and introduced into the conventional primary frequency control. The new primary frequency response characteristic is derived and an order reduction method for frequency-domain transfer function is proposed. Based on this, the time-domain frequency response characteristic is derived and incorporated into the robust look-ahead dispatch model.

Compared to conventional method, it can be seen from the simulation results that the system primary frequency response characteristics could be greatly improved, and hence a higher penetration level of renewable resources could be integrated with the proposed method.

The rest of this paper is organized as follows: Section II describes the proposed primary frequency characteristic with proportional-differential controller and the order reduction method for it. The time-domain frequency response characteristic is also derived. Section III presents the detailed expression of the robust look-ahead dispatch model, in which primary frequency response constraints are formulated. Section IV gives the numerical test on IEEE RTS system. Section V concludes the paper.

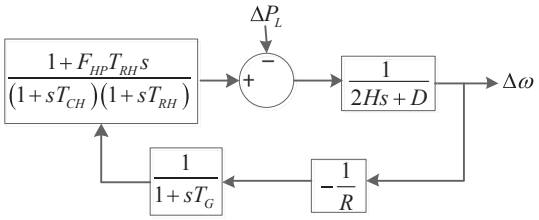

Fig. 1. Conventional primary frequency response of power system.

2. Primary frequency response with proportional-differential controller design

The conventional primary frequency response of power system can be depicted by Fig. 1 and (1).

$$\frac{\Delta\omega}{\Delta P_L} = -\frac{1}{2Hs + D + \frac{(1 + F_{HP}T_{RH}s)}{R(1+sT_G)(1+sT_{CH})(1+sT_{RH})}} \tag{1}$$

where, H represents system inertia constant, D is the load damping rate, $\triangle\mathbf{P_L}$ is the power imbalance disturbance, R is the governor droop rate, T_{RH} is the reheater time constant, F_{HP} is the power fraction of HP turbine to the total turbine power, T_G is the servo motor time constant; T_{CH} is the time constant of the steam chamber and main inlet.

As is known, when there is a generator trip or sudden wind power output fluctuation, the active power balance of the power system will be broken and the frequency will rise or fall correspondingly. When the frequency goes beyond the security range, the power system will become unstable. To avoid this, more inertia or less wind power output is required, resulting in large amount of wind power abandoned sometimes, which reduces the economics of the power system greatly.

If the primary frequency response characteristics can be improved, which means that the amplitude of the frequency fluctuation under contingency could be decreased, e.g. from -0.5 Hz to -0.2 Hz, then more serious disturbances can be withstood by the power system, and more wind power output can be absorbed, which will make the power system more economic.

In this paper, a proportional-differential controller is added as feedback loop to the conventional primary frequency control, and the new primary frequency control procedure is shown in Fig. 2.

The transfer function expression of Fig. 2 is shown in (2).

$$\frac{\Delta\omega}{\Delta P_L} = -\frac{1}{2Hs + D + \frac{(1 + F_{HP}T_{RH}s)}{R(1+sT_{CH})(1+sT_{RH})(1 - R_P + sT_G - sR_D)}} \tag{2}$$

where, R_P and R_D are respectively the proportional and differential coefficient of the feedback loop.

As T_{CH} usually takes the value of 0.2–0.3 s and T_{RH} takes the value of 6–12 s, T_{CH} can be ignored compared to T_{RH} [19]. And the transfer function (2) can be reduced to be (3), whose characteristic polynomial equation is cubic.

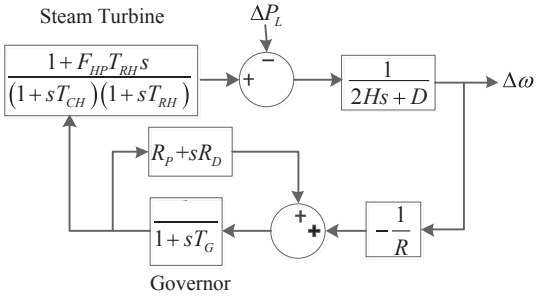

Fig. 2. Proposed primary frequency control with PD feedback.

$$\frac{\Delta\omega}{\Delta P_L} = -\frac{R(1+sT_{RH})(1-R_P+sT_G-sR_D)}{R(2Hs+D)(1+sT_{RH})(1-R_P+sT_G-sR_D)+(1+F_{HP}T_{RH}s)} \tag{3}$$

To make the control system stable, the pole point of the transfer function should be at the left half of the coordinate plane. From Routh-Hurwitz stability criterion, (4)–(7) should be satisfied.

$$2HRT_{RH}(T_G-R_D)>0 \tag{4}$$

$$2HT_{RH}R(1-R_P)+R(2H+T_{RH}D)(T_G-R_D)>0 \tag{5}$$

$$DR(1-R_P)+1>0 \tag{6}$$

$$\left(\frac{1-R_P}{T_G-R_D}+\frac{1}{T_{RH}}+\frac{D}{2H}\right)((2H+T_{RH}D)R(1-R_P)+D(T_G-R_D)R + F_{HP}T_{RH}) > DR(1-R_P)+1 \tag{7}$$

From (4)–(6), it can be deducted that:

$R_D < T_G$ and $R_P < 1+\min\left(\frac{1}{DR}, \left(\frac{1}{T_{RH}}+\frac{D}{2H}\right)(T_G-R_D)\right)$.

When R_P and R_D becomes smaller, the pole point will be farther away from the virtual axis of the coordinate plane, and the control system is stabler. However, the control effect will be poorer, which means that the frequency fluctuation will be larger, and vice versa. Hence, to make the frequency fluctuation small, a larger R_P and R_D should be chosen; meantime, as R usually takes the value of 10^{-3}, both $R(1-R_P)$ and $(T_G-R_D)R$ will be very small. Based on this, (7) can be simplified to be (8) by omitting the small $R(1-R_P)$ and $(T_G-R_D)R$ terms.

$$\frac{1-R_P}{T_G-R_D} > \frac{1}{F_{HP}T_{RH}}-\frac{1}{T_{RH}}-\frac{D}{2H} \tag{8}$$

When T_{RH} takes the typical value of 6–12 s, F_{HP} takes 0.1–0.6, D takes 1% and H takes 3–6 s, it can be deducted from (8) that

$$\frac{T_G-R_D}{1-R_P} < \min\left(\frac{1}{\frac{1}{F_{HP}T_{RH}}-\frac{1}{T_{RH}}-\frac{D}{2H}}\right) \approx 0.71 \tag{9}$$

Based on (9), (3) can be simplified to be (10) by ignoring the smaller time constant $\frac{T_G-R_D}{1-R_P}$ as insignificant compared to T_{RH}.

$$\frac{\Delta\omega}{\Delta P_L} = -\frac{R(1-R_P)(1+sT_{RH})}{R(1-R_P)(2Hs+D)(1+sT_{RH})+(1+F_{HP}T_{RH}s)} \tag{10}$$

When multiple-machine system is considered, (10) can be extended to be (11).

$$\frac{\Delta\omega}{\Delta P_L} = -\frac{1}{(2Hs+D)+\sum_{i=1}^{N}\frac{1+F_{HP,i}T_{RH,i}s}{R_i(1+sT_{RH,i})(1-R_{P,i})}} \tag{11}$$

As the largest frequency dip is less sensitive to the governor time constant $T_{RH,i}$, equal values of T can be assumed for $T_{RH,i}$ from [15]. Meantime, for simplicity, we assume that all of the $R_{P,i}$ take the same value of R_P. Then the transfer function (11) can be rewritten as the following standard form:

$$\frac{\Delta\omega}{\Delta P_L} = -\frac{1+sT}{2HT(s^2+2\varsigma\omega_n s+\omega_n^2)} \tag{12}$$

where

$$\omega_n = \sqrt{\frac{D+\frac{1}{1-R_p}\sum_{i=1}^{N}\frac{1}{R_i}}{2HT}}$$

$$\varsigma = \frac{2H+DT+\frac{T}{1-R_p}\sum_{i=1}^{N}\frac{F_{HP,i}}{R_i}}{2\sqrt{2HT\left(D+\frac{1}{1-R_p}\sum_{i=1}^{N}\frac{1}{R_i}\right)}}$$

The time-domain step response can be derived as

$$\Delta\omega(t) = -\frac{\Delta P_L}{2HT\omega_n^2}\left[1+\alpha e^{-\varsigma\omega_n t}\sin(\omega_n\sqrt{1-\varsigma^2}t+\phi)\right] \tag{13}$$

where $\alpha = \sqrt{\frac{1-2T\varsigma\omega_n+T^2\omega_n^2}{1-\varsigma^2}}$,

$\phi = \arctan\left(\frac{\omega_n\sqrt{1-\varsigma^2}T}{1-\varsigma\omega_n T}\right)-\arctan\left(\frac{-\sqrt{1-\varsigma^2}}{\varsigma}\right)$

Letting the derivative of $\Delta\omega(t)$ equal 0, the extreme point can be obtained.

$$\Delta\omega(t_0) = -\frac{\Delta P_L}{D+\frac{1}{1-R_p}\sum_{i=1}^{N}\frac{1}{R_i}}\left(1+e^{-\varsigma\omega_n t_0}\sqrt{\frac{T}{2H(1-R_p)}\sum_{i=1}^{N}\frac{1-F_{HPi}}{R_i}}\right) \tag{14}$$

where $t_0 = \frac{1}{\omega_n\sqrt{1-\varsigma^2}}\arctan\left(\frac{\omega_n\sqrt{1-\varsigma^2}}{\varsigma\omega_n-1/T}\right)$.

3. Robust look-ahead dispatch model accounting for improved primary frequency response

A robust interval wind power dispatch method is proposed in our previous work [10] to manage operational uncertainties inherent to wind power, in which the impact of worst-case wind power output to transmission interface flow and spinning reserve constraints is considered. In this paper, the proposed primary frequency response is formulated as a constraint and included into the model to account for frequency security of the power system.

1) Objective function

The thermal unit operation cost and the wind power curtailment penalty cost are considered in the objective function.

$$f(p_{it},\bar{\hat{p}}_{jt}^{w},\underline{\hat{p}}_{jt}^{w}) = \left(\sum_{t=t_0+1}^{t_0+T}\sum_{i\in G_{con}}(a_i p_{it}^2+b_i p_{it}+c_i) + \sum_{j\in G_{wind}}\lambda_j((p_{jt}^{w}-\bar{\hat{p}}_{jt}^{w})^2+(\underline{p}_{jt}^{w}-\underline{\hat{p}}_{jt}^{w})^2)\right) \tag{15}$$

where a_i, b_i, c_i are the cost coefficients of thermal unit i. λ_j is the penalty coefficient of wind curtailment, p_{it} is the power output of unit i during time period t. t_0 and T are respectively the initial period and optimization horizon. $[\underline{\hat{p}}_{jt}^{w}, \bar{\hat{p}}_{jt}^{w}]$ is the output schedule of wind farm j during time period t. $[\underline{p}_{jt}^{w}, \bar{p}_{jt}^{w}]$ is the predicted wind power output interval of wind farm j during time period t.

2) Constraints

a) The worst-case frequency response limit constraint

$$\begin{cases}\max\limits_{\Delta p_{jt}^{w}}\left|\frac{\Delta p_{jt}^{w}}{D+\frac{1}{1-R_p}\sum_{i=1}^{N}\frac{1}{R_i}}\left(1+e^{-\varsigma\omega_n t_0}\sqrt{\frac{T}{2H(1-R_p)}\sum_{i=1}^{N}\frac{1-F_{HPi}}{R_i}}\right)\right| \leqslant \Delta\bar{f} \\ \text{s.t.} \quad -1 \leqslant \Delta p_{jt}^{w}/(\bar{\hat{p}}_{jt}^{w}-\underline{\hat{p}}_{jt}^{w}) \leqslant 1 \\ -\Gamma \leqslant \sum_{j}\Delta p_{jt}^{w}/(\bar{\hat{p}}_{jt}^{w}-\underline{\hat{p}}_{jt}^{w}) \leqslant \Gamma\end{cases} \tag{16}$$

where, $\Delta\bar{f}$ is the frequency security threshold of the power system. $\Gamma \in [0,1]$ is the budget of uncertainty, which represents the trade-off of security and economics. The bigger Γ is, the more conservative the result is, and vice versa. Δp_{jt}^{w} is the wind power output fluctuation.

The objective of (16) makes sure that the amplitude of the largest frequency dip under any wind power output scenario is smaller than the allowed frequency security threshold. The first constraint of (16) represents the limit constraint of wind power variation for single wind farm j during time period t. The second constraint of (16) represents the limit constraint of wind power variation for all the wind farms.

(16) is a nonlinear programming model, which cannot be directly solved. However, it can be equivalently transformed to be the following two linear programming models by removing the symbol of absolute value.

$$\begin{cases} \max\limits_{\Delta p_{jt}^{w}} \dfrac{\Delta p_{jt}^{w}}{D+\frac{1}{1-R_p}\sum\limits_{i=1}^{N}\frac{1}{R_i}}\left(1+\mathrm{e}^{-\varsigma\omega_n t_0}\sqrt{\dfrac{T}{2H(1-R_p)}\sum\limits_{i=1}^{N}\dfrac{1-F_{HPi}}{R_i}}\right)\leqslant\Delta\bar{f} \\ \text{s.t.} \quad -1\leqslant\Delta p_{jt}^{w}/(\bar{\hat{p}}_{jt}^{w}-\underline{\hat{p}}_{jt}^{w})\leqslant 1 \\ \qquad -\Gamma\leqslant\sum\limits_{j}\Delta p_{jt}^{w}/(\bar{\hat{p}}_{jt}^{w}-\underline{\hat{p}}_{jt}^{w})\leqslant\Gamma \end{cases} \tag{17}$$

$$\begin{cases} \max\limits_{\Delta p_{jt}^{w}} \dfrac{-\Delta p_{jt}^{w}}{D+\frac{1}{1-R_p}\sum\limits_{i=1}^{N}\frac{1}{R_i}}\left(1+\mathrm{e}^{-\varsigma\omega_n t_0}\sqrt{\dfrac{T}{2H(1-R_p)}\sum\limits_{i=1}^{N}\dfrac{1-F_{HPi}}{R_i}}\right)\leqslant\Delta\bar{f} \\ \text{s.t.} \quad -1\leqslant\Delta p_{jt}^{w}/(\bar{\hat{p}}_{jt}^{w}-\underline{\hat{p}}_{jt}^{w})\leqslant 1 \\ \qquad -\Gamma\leqslant\sum\limits_{j}\Delta p_{jt}^{w}/(\bar{\hat{p}}_{jt}^{w}-\underline{\hat{p}}_{jt}^{w})\leqslant\Gamma \end{cases} \tag{18}$$

b) The power output limit constraints for wind farms and thermal units

$$\hat{p}_{jt}^{w}\leqslant\bar{p}_{jt}^{w} \tag{19}$$

$$\underline{\hat{p}}_{jt}^{w}\leqslant\underline{p}_{jt}^{w} \tag{20}$$

$$\underline{p}_i\leqslant p_{i,t}\leqslant\bar{p}_i \tag{21}$$

where, $\underline{p}_i$, $\bar{p}_i$ are the lower and upper power output limit of unit i.

c) The spinning reserve constraints under worst-case scenarios

$$\begin{cases} \min\limits_{p_{jt}^{w}}\left(\sum\limits_{i\in G_{con}}p_{i,t}+\sum\limits_{i\in G_{con}}R_{it}^{u}+\sum\limits_{j\in G_{wind}}p_{jt}^{w}-D_t\right)\geqslant 0 \\ \quad s.t. \quad \underline{\hat{p}}_{jt}^{w}\leqslant p_{jt}^{w}\leqslant\bar{\hat{p}}_{jt}^{w} \qquad \forall j\in G_{wind} \end{cases} \tag{22}$$

$$\begin{cases} \min\limits_{p_{jt}^{w}}\left(D_t-\sum\limits_{i\in G_{con}}p_{i,t}+\sum\limits_{i\in G_{con}}R_{it}^{d}-\sum\limits_{j\in G_{wind}}p_{jt}^{w}\right)\geqslant 0 \\ \quad s.t. \quad \underline{\hat{p}}_{jt}^{w}\leqslant p_{jt}^{w}\leqslant\bar{\hat{p}}_{jt}^{w} \qquad \forall j\in G_{wind} \end{cases} \tag{13}$$

where, D_t is the load demand of the power system. R_{it}^{u} and R_{it}^{d} are the upward and downward spinning reserve of unit i during time period t, where

$$R_{it}^{u}\leqslant\min(\bar{p}_i-p_{it},\Delta pu_i\Delta T)$$

$$R_{it}^{d}\leqslant\min(p_{it}-\underline{p}_i,\Delta pd_i\Delta T)$$

d) The transmission interface flow constraints under worst-case scenarios

$$\begin{cases} \max\limits_{p_{jt}^{w}}\left(\sum\limits_{i\in G_{con}}(k_{li}p_{it})+\sum\limits_{j\in G_{wind}}(k_{lj}p_{jt}^{w})\right)\leqslant T\bar{L}_l \\ \quad s.t. \quad \underline{\hat{p}}_{jt}^{w}\leqslant p_{jt}^{w}\leqslant\bar{\hat{p}}_{jt}^{w}, \quad l=1,\cdots L \end{cases} \tag{24}$$

$$\begin{cases} \min\limits_{p_{jt}^{w}}\left(\sum\limits_{i\in G_{con}}(k_{li}p_{it})+\sum\limits_{j\in G_{wind}}(k_{lj}p_{jt}^{w})\right)\geqslant T\underline{L}_l \\ \quad s.t. \quad \underline{\hat{p}}_{jt}^{w}\leqslant p_{jt}^{w}\leqslant\bar{\hat{p}}_{jt}^{w} \end{cases} \tag{25}$$

where, $[T\underline{L}_l, T\bar{L}_l]$ represents the transmission interface flow limit. k_{li} is the generation distribution shift factor of unit i to transmission interface l [20].

e) The ramping rate constraint is

$$p_{i,t-1}-\Delta pd_i\Delta T\leqslant p_{it}\leqslant p_{i,t-1}+\Delta pu_i\Delta T \tag{26}$$

The proposed model is a two-layer nonlinear robust optimization problem, which can be transformed into the conventional quadratic programming problem using strong duality theory [10]. And the numerical simulation results are listed as follows.

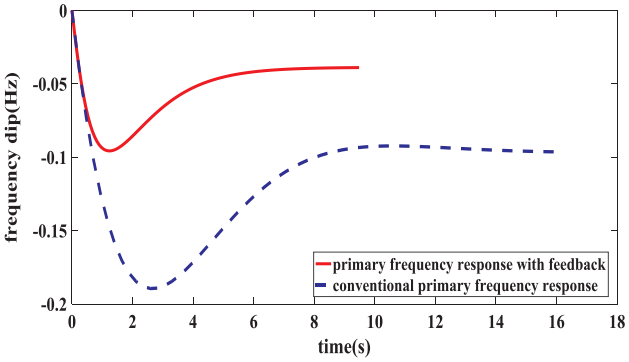

Fig. 3. Primary frequency control effect of the conventional PFC and PFC with PD feedback.

4. Simulation results

In this section, the robust look-ahead dispatch method accounting for improved primary frequency response is tested on the IEEE RTS system [21,22]. And the predicted load demand data is taken from [10]. The predicted wind power output data is shown in Fig. 10.

4.1. The control effects of primary frequency response with and without PD feedback function

Fig. 3 presents the primary frequency response (PFC) curves with and without proportional-differential feedback loop, where the proportional coefficient $R_P = 0.6$ and the differential coefficient $R_D = 0.15$, $T_G = 0.2$ s. And a 23.91 MW sudden decrease in the wind power output, known as wind gust, is considered as a contingency at time 0 s due to its unpredictability.

It can be seen from Fig. 3 that the largest frequency dip is about −0.19 Hz, which occurs at about 2.82 s with the conventional primary frequency control model. This has gone beyond the frequency security range, which is about 0.15 Hz in China and the system will become unstable.

However, when the proportional-differential feedback is considered, the largest frequency dip becomes −0.095 Hz at about 1.20 s, which is still within the frequency security range. Therefore, the PFC with PD feedback could effectively reduce the largest frequency dip and meantime shortening the fluctuation time, which is very beneficial for the transient stability of the power system.

4.2. Comparison of the effects of differential feedback and proportional feedback

The primary frequency response curves with different proportional feedback coefficients (where differential coefficient $R_D = 0.15$) and differential feedback coefficients (where proportional coefficient $R_P = 0.6$) are respectively shown in Figs. 4 and 5.

From the results, it is observed that the proportional coefficient R_P is the dominant factor for the amplitude of the largest frequency dip and the response speed. While the differential feedback coefficient R_D mainly plays the role of oscillation suppression. When R_P becomes larger, the largest frequency dip becomes smaller, and the primary frequency response is faster. When R_D become larger, the amplitude of frequency oscillation becomes smaller.

The amplitude and occurring time of the largest frequency dip under different R_D and R_P combinations are respectively shown in Figs. 6 and 7, and the conclusion is consistent with the analysis in preceding paragraph.

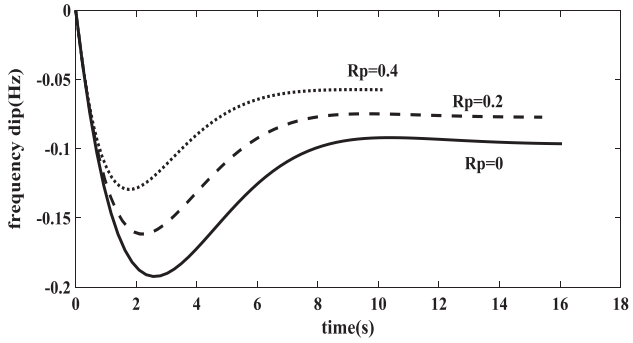

Fig. 4. Primary frequency control effect with different proportional coefficients.

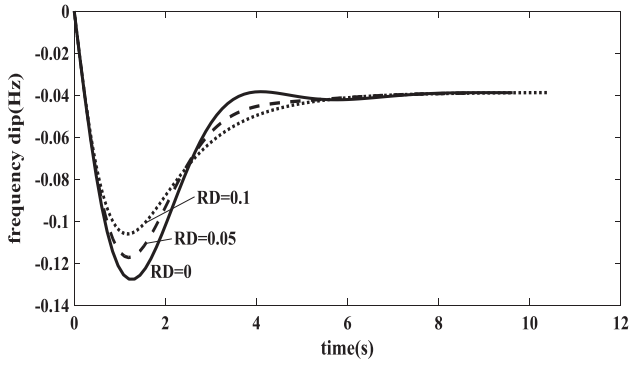

Fig. 5. Primary frequency control effect with different differential coefficients.

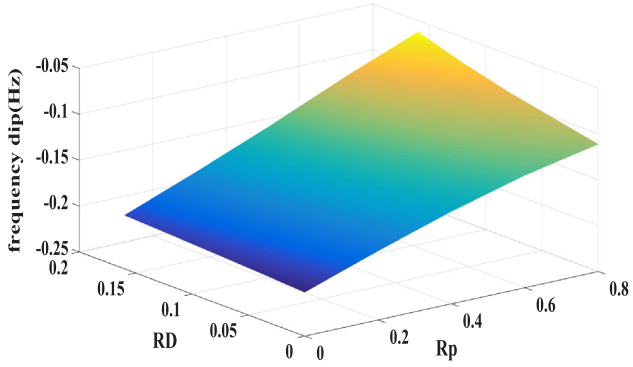

Fig. 6. Amplitude of the largest frequency dip under different R_D and R_P combinations.

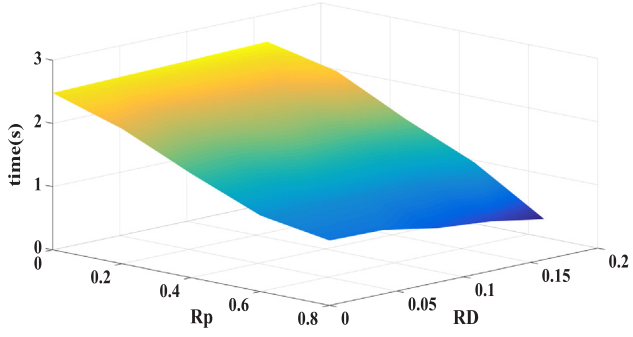

Fig. 7. Occurring time of the largest frequency dip under different R_D and R_P combinations.

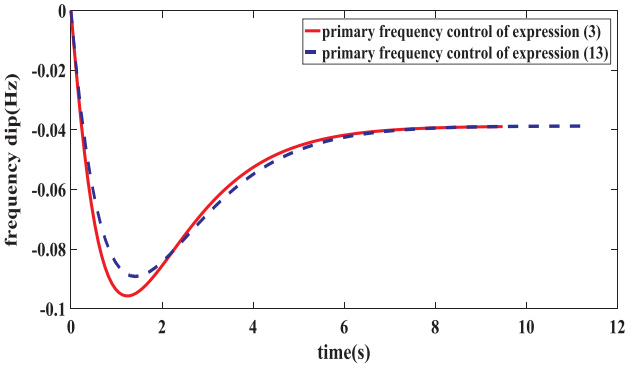

Fig. 8. Comparison of primary frequency control effect between (13) and (3).

4.3. Comparison of simplified time-domain and frequency-domain primary frequency response

Fig. 8 presents the comparison of primary frequency response curve between simplified time-domain expression (13) and frequency-domain expression (3), where $R_P = 0.6$ and $R_D = 0.15$.

From Fig. 8, it's observed that the largest frequency dip is respectively -0.095 Hz and -0.089 Hz with expression (3) and (13). The error is only 0.006 Hz, which is about 6% of the largest frequency dip and is acceptable for onsite use.

The largest frequency dip error curve between simplified time-domain expression (13) and frequency-domain expression (3) under different Rp and R_D combinations is shown in Fig. 9.

It can be seen from Fig. 9 that when R_D is bigger and Rp is smaller, the largest frequency dip error is smaller, and vice versa. When Rp approaches 0 and R_D approaches TG, the error also approaches 0.

4.4. The results of robust look-ahead dispatch accounting for improved primary frequency response

Fig. 10 compares the optimal results of wind power output of robust look-ahead dispatch model with conventional and proposed primary frequency response consideration, where $\Gamma = 0.4$and $\Delta\bar{f} = 0.2$ Hz.

It can be seen from Fig. 10 that:

(1) When the wind power prediction error is small at the beginning time period 1–3, the wind power can be fully absorbed by the power system, and no wind power is curtailed. However, with the increase of wind power prediction error, the absorbed wind power becomes smaller and smaller, and more and more wind power is curtailed.
(2) More wind power can be absorbed during time period 4–7, 8–10 and 11–12 with the proposed primary frequency response model

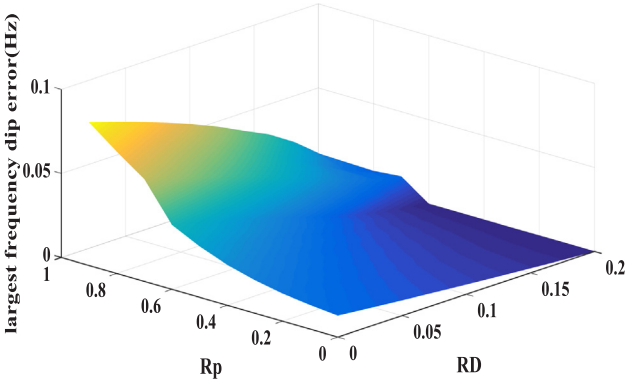

Fig. 9. Comparison of the largest frequency dips error under different Rp and R_D combinations.

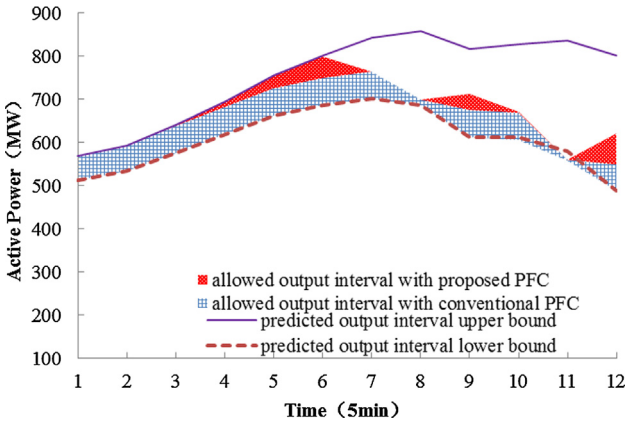

Fig. 10. Comparison of wind power output results of robust look-ahead dispatch method with conventional and proposed primary frequency response consideration.

compared with the conventional primary frequency response model.

Supposing that there is a sudden decrease of wind power output at time interval 6, the worst-case primary frequency response curve of the power system is shown in Fig. 11.

It can be seen that the largest system frequency dip is 0.2 Hz when the primary frequency response is considered in the robust look-ahead dispatch model. However, if the primary frequency response is not considered, the largest system frequency dip will reach 0.37 Hz, which has exceeded the security range and is endangering the power system security.

The upper bound of allowed wind power output interval and the system operation cost with different Γ are respectively shown in Fig. 12 and Table 1, where $\Delta\bar{f} = 0.2$ Hz.

It can be seen that when Γ becomes larger, the system operational cost also becomes larger, while the wind power output interval upper bound becomes smaller. This is consistent with the analysis in section III.

The upper bound of allowed wind power output interval and the system operation cost with different $\Delta\bar{f}$ are respectively shown in Fig. 13 and Table 2, where Γ = 0.4.

It can be seen that when $\Delta\bar{f}$ becomes larger, the system operational cost becomes smaller, while the wind power output interval upper bound becomes larger, which is contrary to the trend of Γ.

5. Conclusion

It is becoming more and more important to consider the frequency security of power system during active power dispatch, especially when large-scale wind power is integrated.

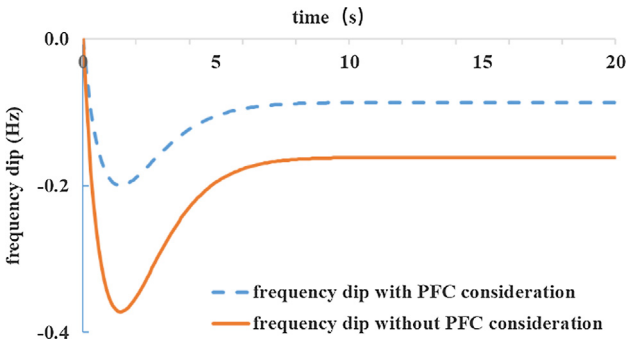

Fig. 11. Comparison of worst-case primary frequency response curve with and without primary frequency response consideration.

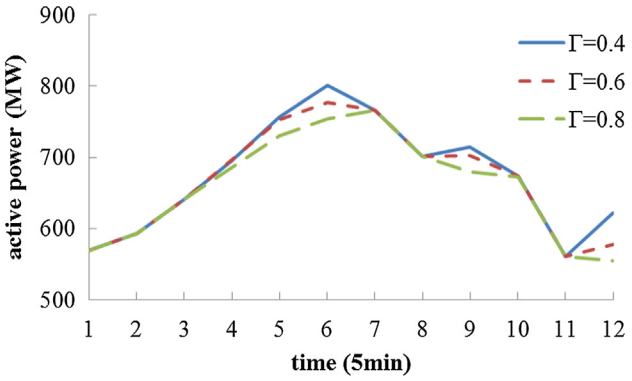

Fig. 12. Wind power output interval upper bound with different Γ.

Table 1
The system operational cost with different Γ.

Γ	0.4	0.6	0.8
cost (10^5\$)	4.1236	4.2275	4.3354

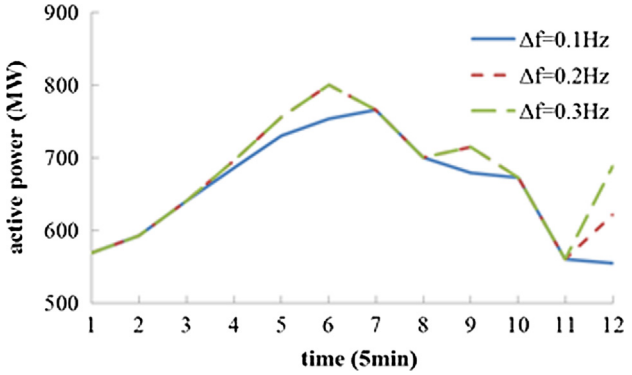

Fig. 13. Wind power output interval upper bound with different $\Delta\bar{f}$

Table 2
The system operational cost with different $\Delta\bar{f}$

$\Delta\bar{f}$	0.1	0.2	0.8
cost (10^5\$)	4.3354	4.1236	4.0218

The existing economic dispatch models with primary frequency response consideration is too conservative, especially for those power systems with large-scale wind power integration, which means that the wind power output will be abandoned severely. This is quite not the expectation of operators and sometimes is even not acceptable.

In this paper, a novel robust look-ahead dispatch method accounting for improved primary frequency response is proposed. The proposed scheme uses the following techniques to overcome shortcomings of the existing algorithms:

(1) A proportional-differential controller is designed and introduced into the conventional primary frequency control loop as a feedback function, and the parameters of which are derived in detail. The controller could effectively improve the primary frequency response characteristics of the power system.
(2) An order reduction method for frequency-domain transfer function is proposed to reduce it from cubic to quadratic. Based on this, the improved time-domain frequency response characteristic is derived.
(3) From the improved time-domain frequency response characteristic, the worst-case frequency response limit constraint is constructed

and incorporated into the robust look-ahead dispatch model, which makes sure that the largest frequency dip under any wind power output scenario is within the security range.

Finally, the simulation is done on IEEE RTS system, and the result proves that the method could effectively improve the frequency response characteristics and a higher penetration level for renewable resources could be integrated compared to the conventional method.

Declaration of Competing Interest

We declare that we have no financial and personal relationships with other people or organizations that can inappropriately influence our work, there is no professional or other personal interest of any nature or kind in any product, service and/or company that could be construed as influencing the position presented in, or the review of, the manuscript entitled.

References

[1] Analysis report on development prospect and investment strategy of China's electric power industry from 2013 to 2018. http://www.askci.com/reports/201210/24154750171930.shtml, accessed 2 December 2018.
[2] Xie Le, Ilic Marija D. Model predictive economic/environmental dispatch of power systems with intermittent resources. IEEE power & energy society general meeting, Calgary, AB, Canada, July 2009.
[3] Gu Y, Xie L. Early detection and optimal corrective measures of power system insecurity in enhanced look-ahead dispatch. IEEE Trans Power Syst 2013;28(2):1297–307.
[4] Xie L, Xu L, Obadina O. Look-ahead dispatch in ERCOT: Case study. In: Proc. 2011 power and energy society general meeting, San Diego, C.A.; 2011. p. 1–3.
[5] Tong Jianzhong, Ni Hui. Look-ahead multi-time frame generator control and dispatch method in PJM real time operations. IEEE power and energy society general meeting, Detroit, MI, USA, July 2011. p. 24–9.
[6] Zhu Yuqi, Chen Yonghong. Modeling short-term Stored Energy Resources under real time look-ahead dispatch on energy and ancillary service market. Cleveland, OH, USA: IEEE Energytech; 2012.
[7] Hoke Anderson, Brissette Alexander, Chandler Shawn, et al. Look-ahead economic dispatch of microgrids with energy storage using linear programming. In: 1st IEEE conference on technologies for sustainability (SusTech), Portland, OR, USA, Aug; 2013.
[8] Xiao Ying, Qianli Su, Wang Xing, et al. Impact of price responsive demand on PJM Real-time/Look-ahead markets. San Diego, CA, USA: IEEE Power and Energy Society General Meeting; July 2011.
[9] Ben-Tal A, Nemirovski A. Robust convex optimization. Math Oper Res 1998;23:769–805.
[10] Wu WC, Chen JH, Zhang BM, et al. A robust wind power optimization method for look-ahead power dispatch. IEEE Trans Sustainable Energy 2014;5(2):507–15.
[11] Li Zhigang, Wu Wenchuan, Zhang Boming, et al. Robust look-ahead power dispatch with adjustable conservativeness accommodating significant wind power integration. IEEE Trans Sustainable Energy 2015;6(3):781–90.
[12] Li Peng, Danwen Yu, Yang Ming, et al. Flexible look-ahead dispatch realized by robust optimization considering CVaR of wind power. IEEE Trans Power Syst 2018;33(5):5330–40.
[13] Lorca Álvaro, Sun Xu Andy. Adaptive robust optimization with dynamic uncertainty sets for multi-period economic dispatch under significant wind. IEEE Trans Power Syst 2015;30(4):1702–13.
[14] Doherty R, Lalor G, O' Malley M. Frequency control in competitive electricity market dispatch. IEEE Trans Power Syst 2005;20(3):1588–96.
[15] Ahmadi H, Ghasemi H. Security-constrained unit commitment with linearized system frequency limit constraints. IEEE Trans Power Syst 2014;29(4):1536–45.
[16] Molina-García Angel, Muñoz-Benavente Irene, Hansen Anca D, et al. Demand-side contribution to primary frequency control with wind farm auxiliary control. IEEE Trans Power Syst 2014;29(5):2391–9.
[17] Restrepo JF, Galiana FD. Unit commitment with primary frequency regulation constraints. IEEE Trans Power Syst 2005;20(4):1836–42.
[18] Teng Fei, Trovato Vincenzo, Strbac Goran. Stochastic scheduling with inertia-dependent fast frequency response requirements. IEEE Trans Power Syst 2016;31(2):1–10.
[19] Anderson PM, Mirheydar M. A low-order system frequency response model. IEEE Trans Power Syst 1990;5(3):720–9.
[20] Sun HB, Zhang BM. A systematic analytical method for quasi-steady-state sensitivity. Electr Power Syst Res 2002;63:141–7.
[21] Wang SJ, Shahidehpour SM, Kirschen DS, et al. Short-term generation scheduling with transmission and environmental constraints using an augmented lagrangian relaxation. IEEE Trans Power Syst 1995;10(3):1294–301.
[22] A report prepared by the reliability test system task force of the application of probability methods subcommittee: 'IEEE reliability test system'. IEEE Trans Power Apparatus and Syst, 1979;98(6):2047–54.